

Interfacial Rheology Through Microfluidics

Jeffrey D. Martin,* Joie N. Marhefka, Kalman B. Migler, and Steven D. Hudson*

The bulk properties and structural characteristics of emulsions arise substantially from their interfacial rheology, which depends strongly on surfactant mass transfer and its coupling to flow. Typical methods used to measure such properties often employ simpler flows and larger drops than those encountered in typical processing applications. Mass transfer mechanisms are governed by droplet size; therefore experimentation at length scales typical of those encountered in applications is desired. Utilizing a microfluidic approach allows high-throughput experimentation at relevant length scales and with adjustable flow dynamics. Using a microfluidic device that facilitates the measurement of interfacial tension in two-phase droplet flows, particle tracers are also used to determine the droplet internal circulation velocity as a measure of interfacial mobility. Combining these measurements in a single device, the coupling between interfacial tension, interfacial retardation, and surfactant mass transfer is explored and mass transfer coefficients and interfacial mobility are measured for a two-phase system containing a diffusing surfactant. Such a device is also used to probe the deformability of elastic capsules and viscoelastic biological cells.

This remarkable coupling (the Marangoni effect^[3]) is easily perceived while simply washing dishes in the kitchen sink. Consider the following from Benjamin Franklin's letter to William Brownrigg, November 7, 1773, "In these experiments, one circumstance struck me with particular surprise. This was the sudden, wide and forcible spreading of a drop of oil on the face of the water.... If a drop of oil is put on a polished marble table, or on a looking-glass that lies horizontally, the drop remains in place, spreading very little. But when put on water, it spreads instantly many feet around, becoming so thin as to produce the prismatic colors, for a considerable space, and beyond them so much thinner as to be invisible, except in its effect of smoothing the waves."^[4] Franklin's oil was not a pure oil, such as mineral oil, which sits in a lens on the surface of water, but it was fatty acids, which are surfactants. Why do they calm the waves?

1. Introduction

Susceptibility to perturbation by flow is a distinguishing feature of "complex" fluids and is the source of their unique rheological properties. For this reason, there is great interest in the coupling between flow and structure of complex fluids. In the realm of emulsions, their bulk properties and structural characteristics arise substantially from their interfacial rheology. The interfacial rheology in turn strongly depends on surfactant mass transfer and its coupling to flow. Even in "clean" systems when no surfactant is present, impurities often act as surface-active agents. Their interfacial rheology is the main reason that surfactants are essential in foods, pharmaceuticals, cosmetics, paints, oil recovery, detergency, multiphase reactions and separations, water remediation, refrigeration, fire-fighting foams, etc.

1.1. Interfacial Rheology

In two-phase systems, when surface-active species are present a dynamic coupling between flow and interfacial tension arises.^[1,2]

Lower surface tension is not the answer. If anything, lower tension allows greater roughness. Instead the answer is surface tension gradients, whose forces produce spreading and oppose the motion of waves, which otherwise causes compression and expansion of the fluid surface. Since such motions can induce changes in local surface surfactant concentration and thus interfacial tension, they may be strongly opposed.^[5] Film spreading and wave suppression are but two manifestations of the Marangoni effect. This effect is also profound on small-sized interfaces, yet different surfactant mass transfer processes may be dominant, as will be discussed in the next section.

Another example of the importance of Marangoni effects is in the stability of emulsions and polymer blends. It is well-known that addition of a surfactant to an emulsion (and compatibilizers to polymer blends) acts to inhibit coarsening of the morphology through suppression of droplet coalescence.^[6–11] For droplet coalescence to occur, the continuous fluid between two approaching droplets must drain to a point where random fluctuations and van der Waals forces destabilize the final remaining film. During either drop approach or film drainage, if surfactant is convected from the contact region, a surfactant concentration gradient arises that causes a Marangoni stress that acts tangentially along the interface in the direction opposing the drainage flow.^[6] This stress therefore tends to immobilize the interface and inhibits film drainage and thus coalescence. Similar effects are active in the stabilization of foams. It is important to note that Marangoni effects are present wherever there may be surfactant concentration gradients at an interface.

J. D. Martin,^[+] J. N. Marhefka, K. B. Migler, S. D. Hudson
Complex Fluids Group, Polymers Division
National Institute of Standards and Technology
100 Bureau Dr., Gaithersburg, MD 20899-8542, USA
E-mail: jeffrey.martin@unilever.com; steven.hudson@nist.gov

[+] Present Address: Unilever Research and Development
40 Merritt Blvd., Trumbull, CT, 06611, USA

DOI: 10.1002/adma.201001758

The relative magnitude of these Marangoni stresses depends on several factors concerning surfactant mass transport (convection, bulk and interfacial diffusivity, and interfacial sorption coefficients) and the magnitude of the change in interfacial tension with surfactant concentration. Depending on process conditions, material parameters, and drop size, the relative importance of these factors can vary. Detailed knowledge is crucial in moving toward the goal of precise control of emulsion properties by varying processing conditions.

1.2. Need for Interfacial Rheology at a Small Scale

As mentioned above, surfactant mass transfer is governed by convection, diffusion, and interfacial sorption rates in two-phase systems, and these processes conspire to establish interfacial tension gradients that exert the forces that couple to flow. As a guide to which of these processes is rate limiting, Jin et al.^[12] identified in 2004 an intrinsic length scale

$$R_{D-K} = \frac{D}{\beta \Gamma_{\max}} \quad (1)$$

which is a ratio of surfactant bulk diffusivity D , interfacial adsorption rate constant β , and maximum interfacial concentration Γ_{\max} . For length scales (e.g., drop radii) reasonably larger than R_{D-K} , mass transfer is diffusion limited, and for sizes reasonably smaller, interfacial sorption rates are dominant due to the dynamics of diffusional mass flux and adsorption or desorption to an increasingly small sphere (drop). R_{D-K} is typically 10 to 100's of micrometers, which may be substantially larger than drop sizes in most applications, e.g., those listed in the Introduction. The relevant dynamics in applications are therefore strongly influenced by interfacial kinetics. Ironically, most characterization methods use large-scale drops and surfaces, and so are insensitive to these interfacial rate constants. Although R_{D-K} marks a characteristic size that identifies the significant role of interfacial kinetics when drops have smaller radii, diffusion most often remains important, since diffusion and sorption processes are in series. More correctly, the limiting mechanism of mass transport is then mixed. Jin et al.^[12] conclude that, "...new surface analysis techniques for the study of dynamic surface tension at reduced length scales should allow significant progress in the study of adsorption-desorption barriers." At the very least, it is desirable to measure interfacial tension in surfactant-containing systems for various drop sizes.

2. Microfluidic Tool

While a droplet-based approach to interfacial rheology began decades ago,^[13,14] new capabilities are provided through microfluidic technology. Microfluidic methods offer excellent control over the production of drops,^[15,16] and are suitable for measurements involving smaller drop sizes on the order of or less than R_{D-K} , the significance of which was just highlighted. As with earlier work using larger apparatuses, microfluidic devices using traps^[17] and flow-through schemes^[18,19] have been demonstrated. For characterization of dynamic, two-phase phenomena, flow-through schemes have several advantages, such as the ability

to adjust component concentrations in situ (high throughput), resistance to buoyancy effects, and access to short-time response.

2.1. Microfluidic Design

The essential functions to be performed by an instrument for droplet interfacial rheology are simple: to produce drops, track their movement, and monitor their deformability. As such, particle tracking velocimetry within the drop indicates interfacial mobility or retardation. Deformability and interfacial tension, σ , are evaluated by means of transient droplet deformation using a microfluidic channel design featuring flow-through constrictions and expansions (Figure 1).^[18,19] By measuring

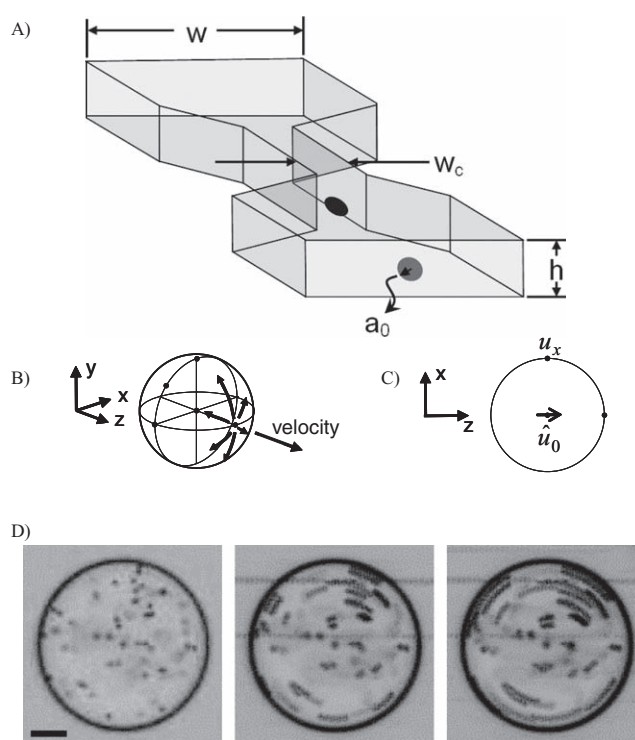


Figure 1. Flow geometry: channel, interfacial flow, and internal drop circulation. a) Schematic geometry of the microfluidic channel. b) Schematic of fountain flow in 3D. The drop velocity is along the z-axis. The velocity of the drop fluid and interface are defined in the drop reference frame. When the interface is fully mobile and the channel is symmetric, the fluid at the drop center moves along the z-axis towards the leading nose, and then passes back toward the rear along the interface as shown schematically by the curved arrows. When the interface is retarded or the channel is asymmetric, other flow patterns occur as described in the text. Points of special interest are marked; in addition to the center and the nose, three other points on the equator (the x-y plane) are shown. c) Schematic of the x-z section of the drop. The flow velocities at the drop center, \hat{u}_0 , and on the interface at extreme x, i.e., \hat{u}_x , are discussed in the text. d) Superposition of images of a droplet flowing in the wide portion of the channel illustrating the internal flow pattern for a water/ethylene glycol drop in silicone oil. The images are taken in the x-z plane (droplet midplane) and the positive z-axis (flow direction) points to the right. Scale bar represents 20 μm , $2a/h = 0.37$, $u_d = 2.9 \text{ mm s}^{-1}$. The time elapsed between images is 0.15 s. As seen from the length of particle streaks and as noted in the text, \hat{u}_0 is here very small and \hat{u}_x is large.

droplet deformation dynamics at channel constrictions, the internal flow patterns and velocities through the use of particle tracers, and the detailed droplet shape, we are able to measure interfacial tension, interfacial rheology, and Marangoni effects, such as interfacial immobilization and non-ideal drop shapes, in the same experiment.

In addition to these basic functions, additional inputs and design features are used to control experimental conditions, such as surfactant concentration or drop composition, tracer-particle concentration, drop spacing, and drop path or streamline. Selection of the streamline and the channel geometry prescribes the local flow kinematics. For example, variations on the channel geometry (height, h , and width, w) and droplet size and position relative to the central axis of the channel allow for variable mixtures of planar extension, and simple and nonlinear shear.^[20] Emulsion processing conditions often involve complex flows, whose coupling with interfacial properties is unclear; specifically, it is not known whether or not the effects of flow complexity are a superposition of simpler effects. Although not explored here, our setup allows for precise control of droplet position within the channel, allowing for precise control of flow complexity.

Channel geometry and operating conditions can be adjusted, as desired, depending on objectives of the measurement, and various fluids and surfactants can be evaluated with this approach. In most, but not all, experiments that we have conducted, the drop is relatively inviscid compared to the surrounding carrier fluid. This arrangement causes measurable drop deformation at relatively lower flow rates,^[19] and it generally forces circulation in the drop. In typical conditions that we have used to measure interfacial mobility and deformability, the capillary number in straight portions of the channel (Poiseuille flow), $Ca_p \approx 10^{-3}$, so that drops are spherical. In the essentially planar extensional flow entering the constriction, the capillary number, $Ca_e \approx 10^{-2}$, so that the interfacial tension may be measured using small deformation theory.^[18,21,22] Also, in our devices the Reynolds number $Re \approx 0.01$ or less. In the following three sections, we will report sample results of interfacial mobility measurements, deformation studies, and modeling.

2.2. Interfacial Mobility

As noted above, surfactant interaction and concentration gradients can act to immobilize the droplet interface.^[1,23–27] To quantitatively measure the extent of interfacial immobilization, polystyrene tracer particles are placed into the droplet phase, facilitating measurement of the internal droplet velocity and flow patterns, which are directly coupled to the interfacial flow. To be passive markers, these particles should be dilute and not adsorb to the interface. Moreover, they should be purified from small molecule impurities. When a droplet travels on the channel centerline, a fountain flow is induced in the drop (Figure 1). The circulation velocity and patterns depend on the relative viscosity of the droplet,^[28,29] and similar effects are expected for varying degrees of interfacial viscosity and immobilization, which can cause drops to behave as if they were more viscous.^[24,25] Thus, these flow patterns can then be compared to theoretical calculations^[30] to quantitatively measure the

extent of interfacial retardation. Theoretically, vector spherical-harmonic functions express these droplet flows.^[31] Remarkably, channel flow excites both dilatational and area-incompressible harmonic modes,^[30] and their magnitude is a direct measure of interfacial mobility to dilation and shear deformation, respectively. This microfluidic approach therefore represents a powerful new interfacial rheology method that will be more fully developed in future reports.

When comparing to theoretical calculations, it is convenient to non-dimensionalize the circulation velocity at any internal point, i , by

$$\hat{u}_i = \frac{u_{ci}/u_d}{(2a/h)^2} \quad (2)$$

where u_{ci} is the velocity of the tracer particle relative to the drop center of mass at point i , u_d is the droplet velocity in the laboratory frame, and $2a/h$ is the degree of confinement.

To approach this topic, the circulation velocity at several points in the drop was measured, e.g., \hat{u}_x (Figure 1) measured at the drop waist in the x - y plane. This was accomplished by near index matching. For aqueous ethylene glycol drops with adventitious surfactant suspended in silicone oil, the central velocity, \hat{u}_0 , was essentially zero (± 0.04), i.e., very severely retarded (a superposition of images taken of a droplet flowing in the wide portion of the channel can be seen in Figure 1d; this illustrates particle tracks and therefore internal circulation). However, the equatorial velocity, \hat{u}_x , was a remarkable 0.41 ± 0.05 (without Marangoni forces \hat{u}_x would be 0).^[30] This indicates that the interfacial shear viscosity is small, since the interfacial mobility to shear is nearly fully mobile^[30] (additional details to be published later). It also indicates that significant changes to circulation patterns may be induced by Marangoni forces, as the relative magnitude of dilatational and shear modes shifts. These little explored shear (area-incompressible) modes are also of interest because, through surfactant diffusion, they may reduce the interfacial concentration gradients and thus couple with dilatational modes and the Marangoni effect. A more complete internal flow profile can be summarized from measurements of internal circulation velocities (non-dimensionalized as in Equation 2) at other positions within the droplet: e.g., \hat{u}_x , \hat{u}_y , and \hat{u}_{xy} for azimuthal angles of 0 , $\pi/2$, and $\pi/4$, respectively (see Figure 1b and c).^[30] With these measurements, the amplitude of the most important spherical-harmonic modes can be determined. The uncertainties reported here, and all uncertainties given, are standard uncertainties from multiple measurements.

As a simpler example, the dimensionless flow rate at the drop center, \hat{u}_0 , has been measured as a function of surfactant concentration (Figure 2) for a system of aqueous, butanol-containing drops in mineral oil.^[20] Since the butanol surfactant undergoes extraction from the drop to the continuous phase, its concentration is time-dependent and is monitored through the instantaneous interfacial tension. For such low-viscosity drops (the ratio of drop to continuous phase viscosity is 0.006) and channel geometry ($w/h = 5$), \hat{u}_0 is equal to 0.5 when the interface is fully mobile.^[30] As we find here, Marangoni effects may be pronounced at low concentrations because they are caused by gradients in surfactant concentration, not just concentration alone. At high concentrations, the interface is remobilized, in

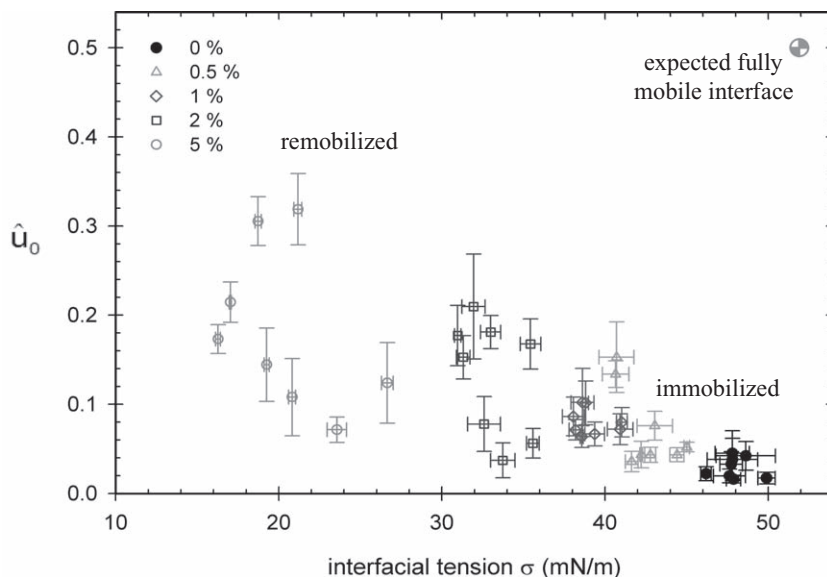


Figure 2. Experimental measurements of \hat{u}_0 in aqueous drops suspended in mineral oil. For fully mobile interfaces, \hat{u}_0 is expected to be 0.5. Severe interfacial retardation is observed, particularly at high interfacial tension (i.e., relatively small interfacial pressure). Substantial remobilization is observed at high surfactant concentration (low tension). Symbols denote butanol surfactant concentration, as noted in the legend upper left. Reproduced with permission.^[20] Copyright 2009, IOP.

accord with more rapid exchange between the interface and the bulk phases, which occurs at higher concentration.^[32]

2.3. Deformability

As mentioned previously, deformability and interfacial tension are evaluated by means of transient droplet deformation facilitated by flow-through constrictions and expansions in a microfluidic channel. Specifically, the interfacial tension is determined by measuring the transient deformation of a droplet entering or exiting a constriction.^[18,19,22] When surfactant transport and sorption occur, the interfacial tension can be monitored as a function of interface age by performing measurements at constrictions and expansions at various points in the channel and at various flow rates (e.g., **Figure 3a**). Octadecyl trimethyl ammonium bromide (C_{18} TAB) is highly surface-active and its adsorption to the interface from very dilute solutions is thus observed in time in a system of aqueous drops in canola oil (**Figure 3a**).

When surfactants are present and drops are under flow, deviations from ellipsoidal drop shapes can occur due to surfactant concentration gradients on the interface.^[24,25] These deviations can be measured using a detailed shape analysis that measures, with subpixel accuracy, the interface position, $R(\theta)$, as a function of polar angle, θ , with respect to the z -axis (see **Figure 1** for corresponding geometry). Errors in $R(\theta)$ on test images were found to be less than one-tenth of a pixel, which translates to about 50 nm at 20x magnification in our experimental setup. Complex shapes can thus be accurately and precisely measured and analyzed during an experiment. For example, using Fourier analysis of $R(\theta)$, the 3rd order component in particular

indicates that a slight bullet-shape distortion may occur when the drop passes through a constriction.

The deformability of elastic capsules and viscoelastic biological cells can also be measured and monitored similarly, since the characteristic surface modulus, defined as the product of the membrane modulus and membrane thickness, acts in the same way that interfacial tension does for liquid drops.^[33–36] For example, a series of images recorded as red blood cells flow through a channel constriction and expansion (**Figure 3b**) can be used to calculate the cell elongation index and fluid extension rate throughout the channel. The elongation index is proportional to the local extension rate of the fluid as the cell approaches the constriction. This measure can be used to characterize the mechanical properties of the red blood cell, and to compare these properties for different cells. For example, we have compared healthy cells to those which have been heated. Heated cells, which are known to be more rigid than normal cells, did not deform as much when they passed through the constriction at the same flow conditions.

In addition, a slight modification of this microfluidic method can also be used to provide mechanical or chemical stresses and exposure times necessary to cause stiffening of the cells, as well as a method to quantify these changes in situ. The timescale of the stiffening process has been difficult to monitor using conventional methods, but microfluidics provides a suitable platform to do so.

2.4. Modeling

As noted above, modeling can translate the above measurements of interfacial mobility and deformation to fundamental material parameters.^[2] By measuring time-dependant interfacial tension, through mass transport of surfactant or changes in interfacial area, etc., a quantitative measure of all four interfacial rate constants for surfactant sorption can be determined, as long as the appropriate equations and conditions are used, e.g., the correct surfactant bulk transport equations and surface equation of state. For example, by measuring the time-dependant interfacial tension (an indirect measure of surfactant concentration) in a microfluidic device with a diffusing surfactant, all four interfacial rate constants for sorption of butanol to the interface between mineral oil and water were quantitatively determined.^[20] The size of the drops being investigated was less than R_{D-K} , thus interfacial kinetics reduced mass transfer rates to approximately an order of magnitude slower than the diffusion limit. In this example, various appropriate assumptions permitted simplification to a one-dimensional spherical model. This one-dimensional model was sufficient to quantitatively determine all four surfactant sorption coefficients.^[20] To model interfacial retardation, however, the model needs to be

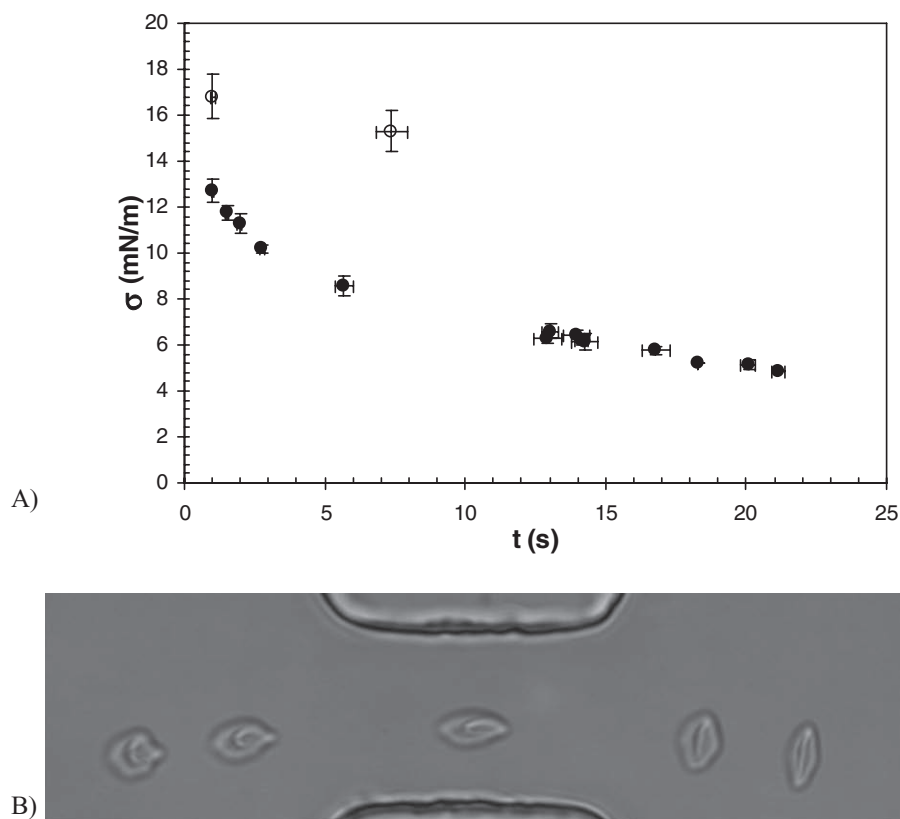


Figure 3. Measurements of the deformability of drops and biological cells. a) Interfacial tension between canola oil and water (with 40 μM , open symbols, and 120 μM , closed symbols, C_{18}TAB surfactant). The tension decreases (increased deformability) with interface age, as C_{18}TAB adsorbs onto the interface. The drop radii are $89 \mu\text{m} \pm 4 \mu\text{m}$ and $97 \mu\text{m} \pm 4 \mu\text{m}$, respectively. b) Superposition of images detailing the deformation of a red blood cell passing through a constriction ($21 \mu\text{m}$ in width). The time interval between images is 0.03 s.

substantially more involved: i.e., 3D and explicitly include convection, e.g., using spherical-harmonic functions. With such a model, interfacial shear and apparent dilatational viscosities will be able to be determined through quantitative comparison to experiment. Since the dilatational mode is coupled to surfactant sorption, mass transfer coefficients may be determined through dilatational measurements by adjusting drop size. In microfluidics, we can also adjust the channel cross section to change the symmetry and observe the effect of Marangoni effects in generating higher-order circulation patterns.

3. Discussion

3.1. Other Methods

As noted above, in general both interfacial shear and dilatational properties are relevant and require different techniques. To measure dilatational and/or surfactant sorption, common techniques measure interface shape (e.g., that of drops distended by gravity^[37,38]) or pressure differences across the interface, for example: growing drop,^[39–42] maximum bubble pressure,^[43–47] or drop volume techniques.^[48] These techniques involve millimeter-sized drops, which are unfortunately often much larger

than R_{D-K} . Some techniques are better suited for liquid-vapor interfaces, but have also been applied to liquid-liquid ones. Typical uses of these techniques are measurement of the static and dynamic surface and interfacial tension. Methods that rely on gravitational forces (pendant drop) suffer from the fact that there must exist a reasonable density difference between the two fluids and an imaging calibration must be performed to eliminate drop-size dependance.^[49] In the maximum bubble pressure method, pressure oscillations must be distinct and large enough to be measured accurately, and systems with small volumes can lead to errors in the measured interfacial tension, and should thus be avoided.^[50] Short-time tension values tend to be overestimated by the drop volume technique; however, corrections exist in the literature.^[50] Quiescent techniques may be able to measure bulk diffusivity and to measure interfacial rate constants in some cases, but they cannot measure coupled flow effects.^[51–53] Such effects have been observed, for example, by Hu and Lips^[23] by using detailed shape analysis (as described above) of droplet deformation between immiscible polymers in a four-roll mill. In this case, the surfactant was insoluble, being formed at, and unable to escape from, the interface. These observations indicated interfacial concentration gradients and were used to measure interfacial tension.

Other rheological methods that measure only interfacial shear viscosity do not introduce interfacial concentration

gradients. For example, Fuller et al. fitted a Langmuir trough with Helmholtz coils and a small magnetic rod that resides at the interface.^[54] Through the force applied on the magnetic rod by the Helmholtz coils and the motion of the rod itself, interfacial rheological properties can be determined. Similarly, interfacial rheology can be performed by probing the diffusion of a microparticle at an interface,^[55–58] and interfacial diffusivity can be determined by fluorescence recovery after photobleaching (FRAP).^[59–61] Interfacial rheology measurements can also be performed at the macroscale: attachments are available (bicone^[62] and ring^[63]) for commercial rheometers that can be placed at liquid-liquid or gas-liquid interfaces.

In regard to two-phase flows in microfluidic devices, while interfacial tension and gradients in interfacial tension play a dominant role in the dynamics of droplet formation,^[15,64–68] only a small number of microfluidic instruments exist that are designed strictly for measuring interfacial tension. Such instruments require calibration and are either based on measuring the frequency of drops produced at a T-junction,^[69] or an adaptation of the drop volume technique.^[70]

3.2. Advantages and Disadvantages of Microfluidic Method

The microfluidic approach for interfacial rheology measurements offers many advantages. For example, device fabrication is relatively cheap, measurements can be performed under (adjustable) flow and at length scales that are relevant for processing applications, multiple inlets allow for the ability to continuously vary component concentration (high throughput), and most importantly, interfacial tension, retardation (viscosity and Marangoni effects), and surfactant mass transfer can be measured in the same experiment.^[20] However, the present microfluidic method cannot easily access as wide a range of time scales as some existing interfacial characterization methods due to the physical constraints of the device (placement of constrictions and overall channel length) and the fact that a flow-through scheme is used.

4. Conclusions

Interfacial rheology can be examined by drop deformation and mobility in a microfluidic platform. Particularly powerful is simultaneous measurement of both interfacial tension and interfacial mobility, because surfactants are used primarily to control these two features. Although a droplet-based approach is decades old, microfluidic technology adds important features, such as control of drop size, interface age, adjustable flow type, and complex flow, that extend this approach. For example, through interfacial age studies and the use of small drops, all of the interfacial sorption rate coefficients in a mineral oil/water/butanol system could be measured.^[20] Although such measurements have been carried out, they are not common because they usually require either very short time resolution or small surface areas so that diffusion does not become the dominant process. The deformability of elastic capsules and viscoelastic biological cells can also be measured and monitored similarly. In such systems, the characteristic surface modulus

acts analogously to interfacial tension in liquid drops. In conclusion, microfluidic methods offer unique, useful, and simple techniques to measure the dynamics of a wide range of systems including two-phase systems, biological cells, and elastic capsules.

Acknowledgements

Funding from the National Research Council (fellowships for JDM and JNM) are gratefully acknowledged. Official contribution of NIST; not subject to copyright in the United States. This article is part of a Special Issue on Materials Science at the National Institute of Standards and Technology (NIST).

Received: May 12, 2010

Published online: August 26, 2010

- [1] H. A. Stone, L. G. Leal, *J. Fluid Mech.* **1990**, 220, 161.
- [2] D. A. Edwards, H. Brenner, D. T. Wasan, *Interfacial transport processes and rheology*, Butterworth-Heinemann, Boston **1991**.
- [3] L. E. Scriven, C. V. Sternling, *Nature* **1960**, 187, 186.
- [4] B. Franklin, in *The writings of Benjamin Franklin, 1773–1776, Vol. 6* (Ed. A. H. Smyth), MacMillan, New York, **1907**, pp 156.
- [5] L. G. Levich, *Physicochemical Hydrodynamics*, Prentice Hall, Englewood Cliffs, NJ **1962**.
- [6] A. K. Chesters, I. B. Bazhlekov, *J. Colloid Interface Sci.* **2000**, 230, 229.
- [7] B. Dai, L. G. Leal, *Phys. Fluids* **2008**, 20, 040802.
- [8] S. D. Hudson, A. M. Jamieson, B. E. Burkhart, *J. Colloid Interface Sci.* **2003**, 265, 409.
- [9] E. Van Hemelrijck, P. Van Puyvelde, C. W. Macosko, P. Moldenaers, *J. Rheol.* **2005**, 49, 783.
- [10] E. Van Hemelrijck, P. Van Puyvelde, S. Velankar, C. W. Macosko, P. Moldenaers, *J. Rheol.* **2004**, 48, 143.
- [11] P. Van Puyvelde, S. Velankar, J. Mewis, P. Moldenaers, *Polym. Eng. Sci.* **2002**, 42, 1956.
- [12] F. Jin, R. Balasubramaniam, K. J. Stebe, *J. Adhes.* **2004**, 80, 773.
- [13] F. Rumschei., S. G. Mason, *J. Colloid Sci.* **1961**, 16, 210.
- [14] F. D. Rumscheidt, S. G. Mason, *J. Colloid Interface Sci.* **1961**, 16, 238.
- [15] S. L. Anna, N. Bontoux, H. A. Stone, *Appl. Phys. Lett.* **2003**, 82, 364.
- [16] T. Thorsen, R. W. Roberts, F. H. Arnold, S. R. Quake, *Phys. Rev. Lett.* **2001**, 86, 4163.
- [17] S. D. Hudson, F. R. Phelan, M. D. Handler, J. T. Cabral, K. B. Migler, E. J. Amis, *Appl. Phys. Lett.* **2004**, 85, 335.
- [18] J. T. Cabral, S. D. Hudson, *Lab Chip* **2006**, 6, 427.
- [19] S. D. Hudson, J. T. Cabral, W. J. Goodrum Jr, K. L. Beers, E. J. Amis, *Appl. Phys. Lett.* **2005**, 87, 081905.
- [20] J. D. Martin, S. D. Hudson, *New J. Phys.* **2009**, 11, 115005.
- [21] J. M. Rallison, *Annu. Rev. Fluid Mech.* **1984**, 16, 45.
- [22] A. Gonzalez-Mancera, in *Mechanical Engineering*, University of Maryland, College Park **2007**.
- [23] Y. T. Hu, A. Lips, *Phys. Rev. Lett.* **2003**, 91, 044501.
- [24] W. J. Milliken, L. G. Leal, *J. Colloid Interface Sci.* **1994**, 166, 275.
- [25] W. J. Milliken, H. A. Stone, L. G. Leal, *Phys. Fluids A* **1993**, 5, 69.
- [26] Y. Pawar, K. J. Stebe, *Phys. Fluids* **1996**, 8, 1738.
- [27] K. J. Stebe, S. Y. Lin, C. Maldarelli, *Phys. Fluids A* **1991**, 3, 3.
- [28] G. Hetsroni, S. Haber, *Rheol. Acta* **1970**, 9, 488.
- [29] A. Nadim, H. A. Stone, *Stud. Appl. Math.* **1991**, 85, 53.
- [30] S. D. Hudson, *Rheol. Acta* **2010**, 49, 237.
- [31] H. S. Lamb, *Hydrodynamics*, Dover publications, New York **1945**.
- [32] K. J. Stebe, C. Maldarelli, *J. Colloid Interface Sci.* **1994**, 163, 177.
- [33] J. D. Wan, W. D. Ristenpart, H. A. Stone, *Proc. Natl. Acad. Sci. USA* **2008**, 105, 16432.

- [34] M. Abkarian, M. Faivre, R. Horton, K. Smistrup, C. A. Best-Popescu, H. A. Stone, *Biomed. Mater.* **2008**, *3*, 034011.
- [35] M. Abkarian, M. Faivre, H. A. Stone, *Proc. Natl. Acad. Sci. USA* **2006**, *103*, 538.
- [36] D. Barthesbiesel, H. Sgaier, *J. Fluid Mech.* **1985**, *160*, 119.
- [37] S. Y. Lin, K. McKeigue, C. Maldarelli, *Langmuir* **1991**, *7*, 1055.
- [38] T. F. Svitova, M. J. Wetherbee, C. J. Radke, *J. Colloid Interface Sci.* **2003**, *261*, 170.
- [39] A. Passerone, L. Liggieri, N. Rando, F. Ravera, E. Ricci, *J. Colloid Interface Sci.* **1991**, *146*, 152.
- [40] C. A. Macleod, C. J. Radke, *J. Colloid Interface Sci.* **1993**, *160*, 435.
- [41] R. Nagarajan, D. T. Wasan, *J. Colloid Interface Sci.* **1993**, *159*, 164.
- [42] L. Liggieri, F. Ravera, M. Ferrari, A. Passerone, R. Miller, *J. Colloid Interface Sci.* **1997**, *186*, 46.
- [43] K. J. Mysels, *Colloids Surf.* **1990**, *43*, 241.
- [44] N. C. Christov, K. D. Danov, P. A. Kralchevsky, K. P. Ananthapadmanabhan, A. Lips, *Langmuir* **2006**, *22*, 7528.
- [45] V. B. Fainerman, V. D. Mys, A. V. Makievski, J. T. Petkov, R. Miller, *J. Colloid Interface Sci.* **2006**, *302*, 40.
- [46] V. B. Fainerman, R. Miller, *J. Colloid Interface Sci.* **1995**, *175*, 118.
- [47] V. B. Fainerman, V. N. Kazakov, S. Lylyk, A. V. Makievski, R. Miller, *Colloids Surf. A* **2004**, *250*, 97.
- [48] R. Miller, A. Hofmann, R. Hartmann, K. H. Schano, A. Halbig, *Adv. Mater.* **1992**, *4*, 370.
- [49] M. C. Yeh, L. J. Chen, *J. Chin. Inst. Chem. Eng.* **2001**, *32*, 109.
- [50] R. Miller, P. Joos, V. B. Fainerman, *Adv. Colloid Interface Sci.* **1994**, *49*, 249.
- [51] J. A. Holbrook, M. D. Levan, *Chem. Eng. Commun.* **1983**, *20*, 191.
- [52] J. A. Holbrook, M. D. Levan, *Chem. Eng. Commun.* **1983**, *20*, 273.
- [53] R. A. Johnson, A. Borhan, *J. Colloid Interface Sci.* **1999**, *218*, 184.
- [54] C. F. Brooks, G. G. Fuller, C. W. Frank, C. R. Robertson, *Langmuir* **1999**, *15*, 2450.
- [55] R. Walder, C. F. Schmidt, M. Dennin, *Rev. Sci. Instr.* **2008**, *79*, 063905.
- [56] M. Sickert, F. Rondelez, H. A. Stone, *EPL* **2007**, *79*, 66005.
- [57] V. Prasad, S. A. Koehler, E. R. Weeks, *Phys. Rev. Lett.* **2006**, *97*, 176001.
- [58] M. Sickert, F. Rondelez, *Phys. Rev. Lett.* **2003**, *90*, 126104.
- [59] O. V. Bychuk, B. Oshaughnessy, *Langmuir* **1994**, *10*, 3260.
- [60] S. H. Kim, H. Yu, *J. Phys. Chem.* **1992**, *96*, 4034.
- [61] E. A. J. Reits, J. J. Neefjes, *Nat. Cell Biol.* **2001**, *3*, E145.
- [62] M. Joly, *Kolloid-Z.* **1939**, *89*, 26.
- [63] S. Vandebriel, A. Franck, G. G. Fuller, P. Moldenaers, J. Vermant, *Rheol. Acta* **2010**, *49*, 131.
- [64] S. L. Anna, H. C. Mayer, *Phys. Fluids* **2006**, *18*, 121512.
- [65] G. F. Christopher, S. L. Anna, *J. Phys. D: Appl. Phys.* **2007**, *40*, R319.
- [66] M. De Menech, P. Garstecki, F. Jousse, H. A. Stone, *J. Fluid Mech.* **2008**, *595*, 141.
- [67] A. S. Utada, A. Fernandez-Nieves, H. A. Stone, D. A. Weitz, *Phys. Rev. Lett.* **2007**, *99*, 094502.
- [68] P. Garstecki, M. J. Fuerstman, H. A. Stone, G. M. Whitesides, *Lab Chip* **2006**, *6*, 437.
- [69] N. T. Nguyen, S. Lassemono, F. A. Chollet, C. Yang, **2006**, World patent 098700 A1.
- [70] J. H. Xu, S. W. Li, W. J. Lan, G. S. Luo, *Langmuir* **2008**, *24*, 11287.